MATERIALS CHEMISTRY FRONTIERS

RESEARCH ARTICLE

View Article Online
View Journal | View Issue

Check for updates

Cite this: *Mater. Chem. Front.*, 2020, **4**, 899

Received 23rd October 2019,
Accepted 18th January 2020

DOI: 10.1039/c9qm00648f

rsc.li/frontiers-materials

Published on 20 2020. Downloaded on 17.10.2024 17:54:35.

# A zinc-responsive fluorophore based on 5′-(*p*-hydroxyphenyl)-pyridylthiazole†

Yuichiro Watanabe,[a] Wanna Sungnoi,[a] Andrew O. Sartorio,[b] Matthias Zeller[a] and Alexander Wei *[ac]

The synthesis and photophysical properties of an ion-sensitive fluorescent compound are described, featuring 5′-(*p*-hydroxyphenyl)pyridylthiazole (HPPT) as a highly emissive fluorophore. Density functional theory (DFT) calculations indicate that HPPT is capable of intramolecular charge transfer (ICT), with further polarization upon complexation with Zn(II). A 4′-picolyloxy–HPPT derivative was prepared and determined to form a 1:1 complex with $Zn(NO_3)_2$ in acetonitrile, with a Stokes shift of 137 nm (6323 $cm^{-1}$) and a 67 nm bathochromic shift in emission relative to the neutral ligand, and a fluorescence quantum yield ($\Phi_{PL}$) of 92%. An X-ray crystal structure of the HPPT–Zn(II) complex confirmed a tridentate structure with a seven-membered chelate ring, and the picolyloxy unit rotated out of plane.

## Introduction

Chemically responsive fluorescent dyes are useful as probes for biological imaging and as components in the design of molecular logic gates.[1–5] In many cases, molecular recognition events can be transduced by fluorescence using photoinduced electron transfer (PET) or intramolecular charge transfer (ICT) mechanisms.[6,7] The latter has been broadly applied toward the design of ratiometric fluorescence sensing modalities that can quantify changes in the concentration of specific analytes.

ICT is commonly observed in π-conjugated systems with electron-rich and electron-poor (donor and acceptor) units at opposite ends of the molecule. If the excited-state dipole is proximal to an ion binding site, then ICT efficiency can be modulated in a supramolecular fashion. For example, acceptor units that can bind metal ions may experience an increased electric polarization upon chelation, causing a bathochromic shift in photoemission (Fig. 1a). Ratiometric fluorescence sensing has been applied successfully toward the detection of transition-metal ions including Zn(II), an essential cofactor in many biological functions.[8–10] The Zn(II) ion is compatible with excited-state processes, and can be incorporated into the design of fluorophores with large Stokes shifts.[11–14]

Several Zn(II)-binding fluorophores are based on well-established dye scaffolds such as BODIPY,[1,15] xanthene,[3,16] and coumarin,[3b,11] which all have high quantum yields ($\Phi_{PL}$) but produce small Stokes shifts upon metal ion binding. Fluorophores containing quinoline units have been shown to respond to Zn(II) with Stokes shifts of over 200 nm (8500 $cm^{-1}$), but are limited by their low $\Phi_{PL}$.[13] These earlier examples set the stage

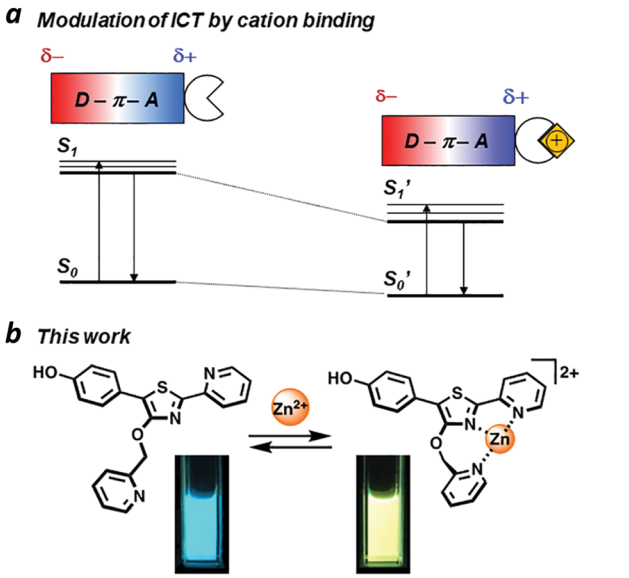


Fig. 1 (a) Intramolecular charge transfer (ICT) within a π-conjugated donor–acceptor system, modulated by ion binding; (b) a Zn(II)-binding fluorophore using 5′-(*p*-hydroxyphenyl)pyridylthiazole (HPPT) as an ICT platform.

[a] *Department of Chemistry, Purdue University, West Lafayette, 560 Oval Drive, Indiana, 47907-2084, USA. E-mail: alexwei@purdue.edu*
[b] *Davidson School of Chemical Engineering, Purdue University, 480 Stadium Mall Drive, West Lafayette, IN 47907-2100, USA*
[c] *School of Materials Engineering, Purdue University, 701 W. Stadium Avenue, West Lafayette, Indiana 47907-2045, USA*

† Electronic supplementary information (ESI) available: Additional DFT calculations and photophysical studies, details on synthesis and X-ray crystallography, and NMR spectra. CCDC 1960137 and 1960138. For ESI and crystallographic data in CIF or other electronic format see DOI: 10.1039/c9qm00648f

Published on 20 2020. Downloaded on 17.10.2024 17:54:35.

for developing new classes of ion-responsive fluorophores, featuring supramolecular binding motifs that have direct impact on their excited-state dipoles.

We have identified 5′-phenyl-2′-(2-pyridyl)thiazole (PPT) as a promising scaffold for the rational design of ratiometric fluorescent probes, using the ICT approach (Fig. 1b). The bidentate cleft of the pyridylthiazole unit can be fashioned into a receptor for transition-metal ions, providing a useful mechanism for lowering the energy of its acceptor state.[17,18] Earlier studies on the chemistry and photophysical properties of 2′-(2-pyridyl)thiazoles by Yan[19] and Beckert[20] have shown these compounds to be capable of supporting high $\Phi_{PL}$ and large Stokes shift due to structural changes in their excited states, with considerable tolerance for chemical modification. Their studies provide an excellent starting point for designing PPT derivatives whose fluorescence outputs can be tuned by well-defined supramolecular interactions. In this paper, we introduce 5′-(*p*-hydroxyphenyl)pyridylthiazole (HPPT) as a highly emissive ICT-type fluorophore, and a Zn(II)-binding HPPT derivative that exhibits a 67 nm bathochromic shift in emission upon complexation, with 92% $\Phi_{PL}$ and a Stokes shift of 137 nm (6323 $cm^{-1}$).

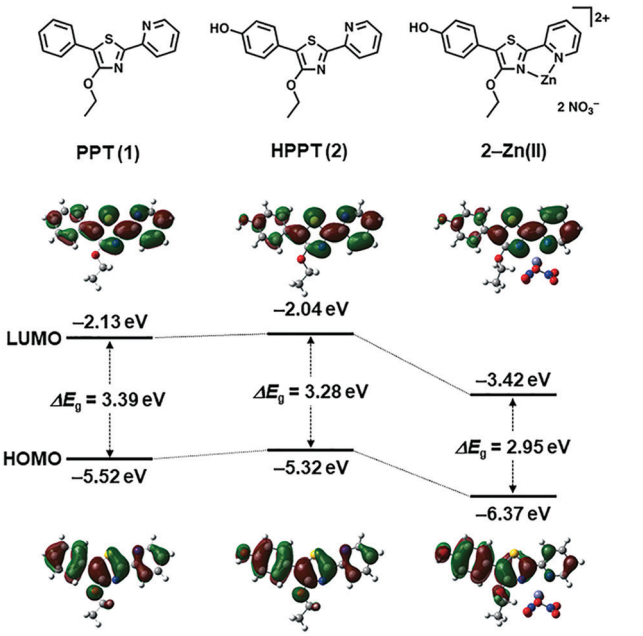


Fig. 2 DFT calculations of energy bands and spatial distributions of molecular orbital coefficients (HOMO and LUMO) for 4′-*O*-Et-PPT (**1**), 4′-*O*-Et-HPPT (**2**), and **2–Zn(II)**. See ESI† for additional DFT calculations.

## Results and discussion

### DFT calculations

To determine the feasibility of generating excited-state ICT within the PPT scaffold, we first conducted density functional theory (DFT) calculations to evaluate the effects of *p*-substitution on the phenyl ring of the PPT unit, with and without Zn(II) complexation.[21] HPPT was selected as an ICT-type fluorophore due to the strong polarization of its molecular orbital (MO) states by the *p*-hydroxyl group, relative to that of unsubstituted PPT (Fig. 2 and ESI†). Coordination between the pyridylthiazole unit and $Zn(NO_3)_2$ further increased polarization of the LUMO coefficients as expected, with the decrease in energy band gap ($\Delta E_g$) being most pronounced for HPPT. We also performed DFT calculations on pyridylthiazole derivatives bearing a picolyloxy group (4′-*O*-Pic-PPT **3** and 4′-*O*-Pic-HPPT **4**), a well-known ancillary ligand for stabilizing Zn(II) binding, and confirmed that its presence had a negligible effect on the spatial distribution of MO coefficients (see ESI†).

### Synthesis

PPT derivatives with a 4′-hydroxyl on the central thiazole ring were prepared using Hantzsch conditions,[22] similar to those described by Beckert and coworkers (Scheme 1).[23,24] In the case of HPPT, ethyl *p*-hydroxyphenylacetate was converted to a pivaloyl ester then brominated at the methylene position, and condensed with 2-pyridylthioamide by microwave heating to yield the corresponding 4′-hydroxythiazole in 25% yield over three steps. *O*-Alkylation with ethyl iodide or picolyl bromide followed by methanolysis produced 4′-*O*-Et-HPPT (**2**) or 4′-*O*-Pic-HPPT (**4**) respectively. PPT derivatives lacking the *p*-hydroxyl group, namely 4′-*O*-Et-PPT (**1**) and 4′-*O*-Pic-PPT (**3**), were prepared according to literature procedure and alkylated as described above.[24]

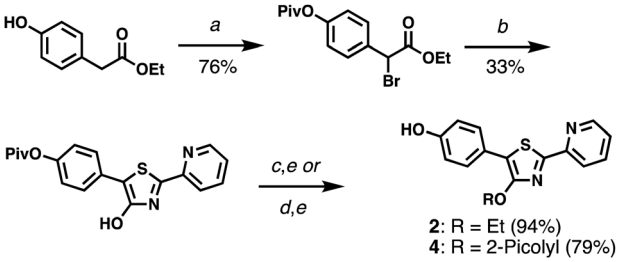


Scheme 1 Synthesis of HPPT derivatives **2** and **4**. (a) (i) PivCl, DMAP, pyridine; (ii) NBS, AIBN, TFT, 80 °C. (b) 2-Pyridylthioamide, EtOH, 90 °C (μW). (c) EtI, $K_2CO_3$, acetone. (d) 2-PicBr·HBr, $K_2CO_3$, acetone. (e) $K_2CO_3$, MeOH. See ESI† for reagent abbreviations.

### X-ray crystal structure determination

The crystal structure of compound **4** revealed the π-conjugated chromophore to be nearly planar (phenyl-thiazolyl dihedral angle = 12.15°; pyridyl-thiazolyl dihedral angle = 7.33°), with the nitrogen atoms adopting a transoid geometry to minimize steric interactions between rings. In contrast, the 4′-*O*-picolyl group is nearly perpendicular with respect to the thiazole ring (Fig. 3a). The crystal structure of complex **4–Zn(II)**, which was prepared by mixing $Zn(NO_3)_2$ with **4** in equimolar ratio, confirmed the tridentate nature of Zn coordination by the 4′-*O*-picolyl unit and the two pyridylthiazole nitrogens in cisoid geometry (Fig. 3b). The bite angles for N1–Zn–N2 and N2–Zn–N3 are 77.8° and 100.2°, respectively. Notably, there are no significant differences in the distances between Zn–N bonds (Zn–N1 bond length = 2.121 Å; Zn–N2 = 2.125 Å; Zn–N3 = 2.110 Å), despite the fact that the pyridine ring in the picolyloxy arm is rotated out of plane by 26.4° relative to the thiazole. The seven-membered

 This journal is © The Royal Society of Chemistry and the Chinese Chemical Society 2020

Published on 20 2020. Downloaded on 17.10.2024 17:54:35.

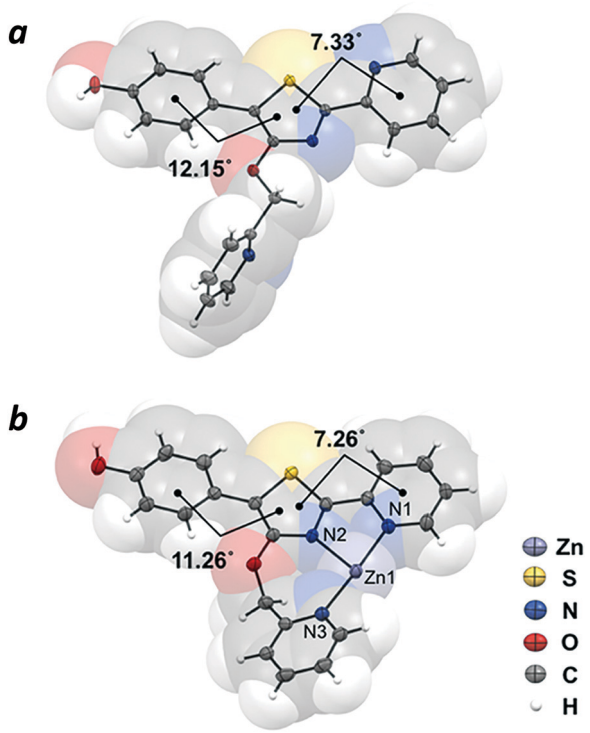


Fig. 3 X-ray crystal structures of (a) 4′-*O*-Pic-HPPT (**4**) and (b) **4–Zn(II)**. Nitrate counterions are omitted for clarity. Thermal ellipsoids are shown at 50% probability.

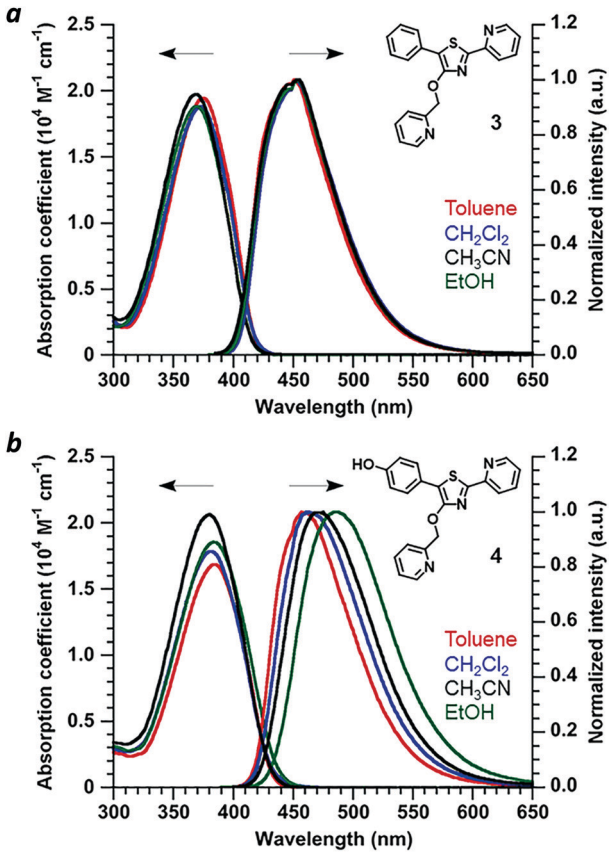


Fig. 4 (a) Optical absorption and normalized PL spectra of 4′-*O*-Pic-PPT **3** and (b) 4′-*O*-Pic-HPPT **4**. Spectra recorded at 30 μM and 20 °C.

chelate ring is uncommon,[25] but may be a useful binding motif in the design of other coordination complexes.

## Photophysical properties

Absorbance and photoluminescence (PL) spectra of 4′-*O*-Pic-PPT **3** and 4′-*O*-Pic-HPPT **4** were acquired in solvents of varying polarity to determine the extent of electric polarization within HPPT (Fig. 4). HPPT **4** has a strong absorption band near 380 nm ($\varepsilon_M$ = 2 × $10^4$ $M^{-1}$ $cm^{-1}$, $CH_3CN$) corresponding with its π–π* transition, and is redshifted by 11 nm relative to that of PPT **3** ($\lambda_{max}$ = 369 nm). **4** also exhibits solvatochromism in its PL spectra, with a shift in peak emission ($\lambda_{em}$) from 461 nm in toluene ($\varepsilon_d$ 2.38) to 487 nm in ethanol ($\varepsilon_d$ 24.5), indicating increased stabilization of its excited-state dipole by a polar environment (see ESI†).[26] Similar phenomena were observed with 4′-*O*-ethyl derivative **2**, validating HPPT as a donor–acceptor ICT system (Table 1 and ESI†). The $\Phi_{PL}$ for all PPT derivatives in acetonitrile are well over 90%, and correlate well with previous studies.[20,23] Optical band gaps ($E_g$) were estimated from the absorption edge to be 3.0 eV for **1** and **3** and 2.9 eV for **2** and **4**, indicating minimal perturbation of the π-conjugated system by the 4′-*O*-alkyl unit.

Coordination of Zn(II) to 4′-*O*-Pic-HPPT **4** led to striking changes in emission colour with retention of high $\Phi_{PL}$ (Table 1). The $\lambda_{em}$ of **4** shifted by 67 nm toward the red upon Zn(II) binding, from 472 to 539 nm. A 22 nm redshift in absorbance ($\Delta\lambda_{max}$) from 380 to 402 nm was also observed, with well-defined isosbestic points at 305 and 393 nm (Fig. 5a). Stoichiometric titration of $Zn(NO_3)_2$ into a $CH_3CN$ solution of **4** produced linear changes in both absorption and emission peak intensities, with no further change after one molar equivalent (Fig. 5b). The association constant ($K_a$) for $Zn^{2+}$ binding by **4** was determined to be 9.6 × $10^7$ $M^{-1}$ (see ESI†), higher than that reported for some similar compounds in $CH_3CN$.[18] In comparison, coordination of Zn(II) to 4′-*O*-Pic-PPT **3** induced much smaller redshifts in emission ($\Delta\lambda_{em}$ = 22 nm) and absorbance ($\Delta\lambda_{max}$ = 14 nm), as well as a slight loss in $\Phi_{PL}$ and a lower $K_a$ value (see ESI†). No redshifts were observed for 4′-*O*-ethyl derivatives **1** or **2**, meaning that the pyridyl nitrogen in the 4′-*O*-picolyl group was necessary for Zn(II) binding, and could adopt an appropriate geometry for stable complex formation. Lastly, exchanging counterions from nitrate to perchlorate or triflate had little effect on the photophysical properties of **4** (see ESI†).

Table 1 Photophysical properties of PPT derivatives (in $CH_3CN$)

| Compound | Abs ($\lambda_{max}$) (nm) | $\varepsilon_M$ × $10^4$ ($M^{-1}$ $cm^{-1}$) | $\lambda_{em}$ [a] (nm) | $\nu_{St}$ ($cm^{-1}$/nm) | $\Phi_{PL}$ [b] (%) |
|---|---|---|---|---|---|
| **1** (4′-*O*-Et-PPT) | 371 | 1.90 | 454 | 4928/83 | 96 |
| **2** (4′-*O*-Et-HPPT) | 383 | 1.77 | 476 | 5101/93 | 96 |
| **3** (4′-*O*-Pic-PPT) | 369 | 1.97 | 454 | 5074/85 | 94 |
| **4** (4′-*O*-Pic-HPPT) | 380 | 2.07 | 472 | 5129/92 | 92 |
| **3–Zn(II)** | 383 | 1.82 | 476 | 5101/93 | 87 |
| **4–Zn(II)** | 402 | 1.85 | 539 | 6323/137 | 92 |

[a] $\lambda_{ex}$ = 370 nm for **1** and **3**, 380 nm for **2** and **4**, 383 nm for **3–Zn(II)**, and 402 nm for **4–Zn(II)**. [b] $\Phi_{PL}$ determined using an integrating sphere.

Published on 20 2020. Downloaded on 17.10.2024 17:54:35.

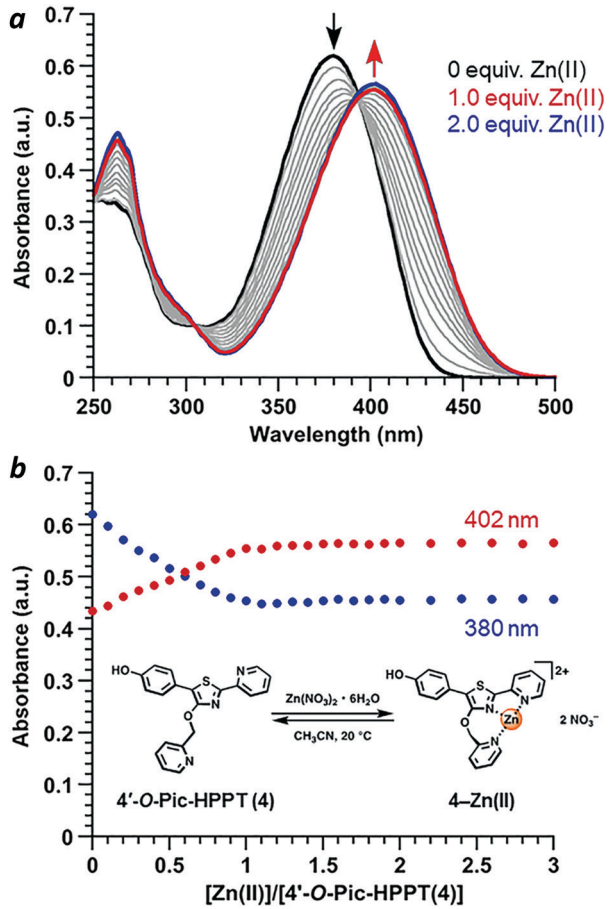


Fig. 5 (a) Spectral changes in the absorbance of **4** (30 μM) upon titration of $Zn(NO_3)_2{\cdot}6H_2O$ (3 mM in $CH_3CN$). (b) Stoichiometry of **4–Zn(II)** complex formation in $CH_3CN$ using the molar ratio method, based on absorbance maxima.

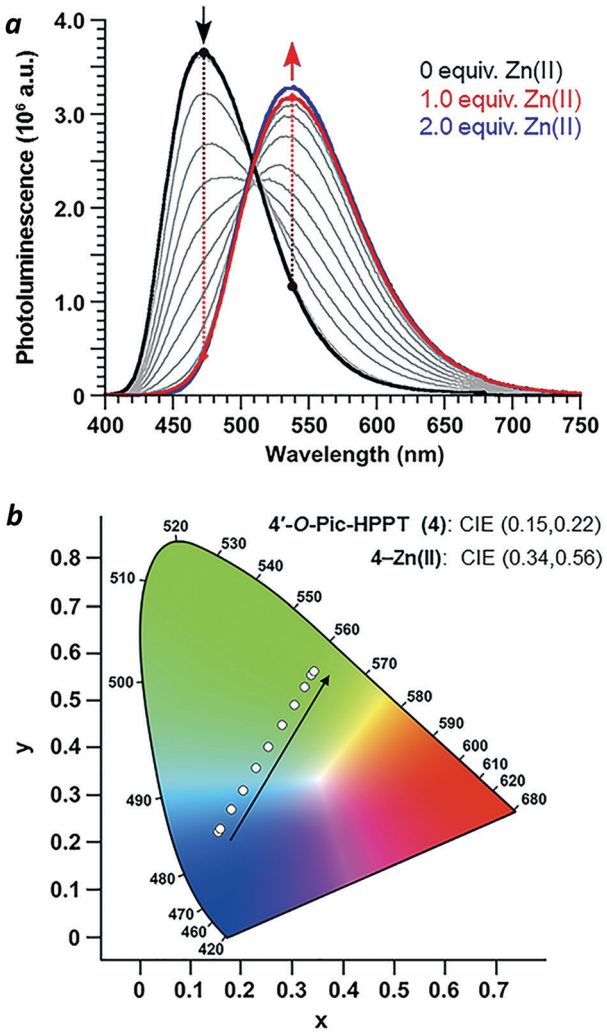


Fig. 6 (a) Spectral changes in the photoluminescence of **4** (30 μM in $CH_3CN$) upon titration of $Zn(NO_3)_2{\cdot}6H_2O$ (3 mM in $CH_3CN$) and excitation at the isosbestic point ($\lambda_{ex}$ = 393 nm). (b) CIE chromaticity diagram of **4** showing the progression in emitted light with $Zn(NO_3)_2$ addition.

With regard to visual perception, HPPT derivatives produce photons that are easily detected by the human eye. The photoluminescence of **4** ($\lambda_{ex}/\lambda_{em}$ = 393/472 nm) corresponds with chromaticity coordinates (0.15,0.22) in Commission Internationale de L'Eclairage (CIE) 1931 colour space (Fig. 6).[27] Formation of the **4–Zn(II)** complex results in a peak emission at 539 nm, which shifts the CIE coordinates to (0.34,0.56) within the green region. To translate these CIE coordinates into an optical readout of Zn(II) binding, the ratio of emission intensities at 539 and 472 nm ($F_{539}/F_{472}$) increases from 0.12 in the absence of Zn(II) to 2.77 in the presence of equimolar Zn(II). This ratiometric increase is greater than 20-fold, and implies that **4** can function as a single-excitation dual-emission probe for Zn(II) at wavelengths appropriate for unaided visual analysis. For comparison, the CIE coordinates for PL emission from PPT derivative **3** ($\lambda_{ex}/\lambda_{em}$ = 377/454 nm) shift in response to Zn(II) from CIE (0.15,0.10) to CIE (0.16,0.25) ($\lambda_{em}$ for **3–Zn(II)** = 476 nm). The ratio of emission intensities ($F_{476}/F_{454}$) changes from 0.72 in the absence of Zn(II) to 1.38 in the presence of equimolar Zn(II), corresponding to less than a 2-fold increase. Moreover, **4–Zn(II)** has a Stokes shift of 137 nm ($\nu_{St}$ = 6323 $cm^{-1}$), whereas that of **3–Zn(II)** is 93 nm or 5101 $cm^{-1}$ (Table 1 and ESI†). The larger Stokes shift reduces the overlap between excitation and emission bands, and minimizes self-quenching.

## Conclusions

5′-(*p*-Hydroxyphenyl)pyridylthiazole is a new ICT-type fluoro-phore that can be configured for a strongly emissive response to Zn(II) ions. The HPPT platform is easy to synthesize and amenable to derivatization, particularly at the 4′ position. The 4′-*O*-picolyl arm stabilizes the coordination of Zn(II), as shown by x-ray crystallography and by the absence of a Zn-induced shift in emission for 4′-*O*-ethyl HPPT **2** in solution. The *p*-hydroxyphenyl unit in Pic-HPPT **4** is responsible for a 67 nm shift in emission upon Zn(II) binding, compared with a 22 nm shift in emission for PPT **3**. The **4–Zn(II)** complex has a relatively large Stokes shift of 137 nm or 6323 $cm^{-1}$, which bodes well for optical sensing and imaging applications. Investigations on the metal-ion binding properties of HPPT derivatives in aqueous solutions are in progress, and will be reported in due course.

 This journal is © The Royal Society of Chemistry and the Chinese Chemical Society 2020

Published on 20 2020. Downloaded on 17.10.2024 17:54:35.

## Experimental

Chemical reagents and supplies obtained from commercial vendors were used as supplied unless otherwise noted. *N*-Bromo-succinimide (NBS) was recrystallized from water as a white crystalline solid. Microwave reactions were performed using a CEM Discovery microwave reactor. $^{1}$H and $^{13}$C NMR spectra were collected at room temperature on a Varian INOVA 300, Bruker AV400 HD, or AV800 HD spectrometer. NMR samples were prepared in chloroform-*d*, acetone-$d_6$, or dimethyl sulfoxide-$d_6$, with chemical shifts ($\delta$) reported in ppm relative to residual solvent resonances as internal standards. Electrospray ionization mass spectra were obtained using an Advion Expression compact spectrometer. Full details on the synthesis and characterization of **1–4** and their intermediates are described in the ESI.†

Absorption spectra were acquired on a Varian Cary50 Bio UV-Vis spectrophotometer using a 1-cm quartz cuvette. Photoluminescence spectra and absolute quantum yields ($\Phi_{PL}$) were measured using an Edinburgh Instruments FLS 980 spectrometer with an integrating sphere accessory. Chromaticity (CIE) coordinates were analysed with F980 software. Quantum chemical calculations were performed using the hybrid density functional theory (DFT) functional (Gaussian 16).[21] Geometries of PPT derivatives were optimized at the B3LYP level using the 6-31+G(d,p) basis set for the ground state. Geometries of PPT–Zn(II) complexes were optimized at the B3LYP/Gen level using the 6-31+G(d,p) basis set for H, C, N atoms and LANL2DZ basis set for the Zn(II) atom in the gas phase. Crystallographic data reported in this paper are tabulated in the ESI† and archived at the Cambridge Crystallographic Data Centre under reference numbers CCDC 1960137 and 1960138.†

## Conflicts of interest

There are no conflicts to declare.

## Acknowledgements

This work was supported by the ACS Petroleum Research Fund (58453-ND4). Y. W. gratefully acknowledges a fellowship provided by the Japan Society for the Promotion of Science (JSPS). Funding for the single crystal X-ray diffractometer was provided by the National Science Foundation (CHE-1625543). We thank Ericka (Kistler) Brandau, Benjamin Washer, Patricia Bishop, and Hartmut Hedderich for technical support.

## References

1 (*a*) A. Loudet and K. Burgess, BODIPY Dyes and Their Derivatives: Syntheses and Spectroscopic Properties, *Chem. Rev.*, 2007, **107**, 4891; (*b*) J. Han and K. Burgess, Fluorescent Indicators for Intracellular pH, *Chem. Rev.*, 2010, **110**, 2709.

2 H. Kobayashi, M. Ogawa, R. Alford, P. L. Choyke and Y. Urano, New Strategies for Fluorescent Probe Design in Medical Diagnostic Imaging, *Chem. Rev.*, 2010, **110**, 2620.

3 (*a*) X. Chen, T. Pradhan, F. Wang, J. S. Kim and J. Yoon, Fluorescent Chemosensors Based on Spiroring-Opening of Xanthenes and Related Derivatives, *Chem. Rev.*, 2012, **112**, 1910; (*b*) D. Cao, Z. Liu, P. Verwilst, S. Koo, P. Jangjili, J. S. Kim and W. Lin, Coumarin-Based Small-Molecule Fluorescent Chemosensors, *Chem. Rev.*, 2019, **119**, 10403.

4 J. Chan, S. C. Dodani and C. J. Chang, Reaction-based small-molecule fluorescent probes for chemoselective bioimaging, *Nat. Chem.*, 2012, **4**, 973.

5 X. Li, X. Gao, W. Shi and H. Ma, Design Strategies for Water-Soluble Small Molecular Chromogenic and Fluorogenic Probes, *Chem. Rev.*, 2014, **114**, 590.

6 (*a*) R. A. Bissell, A. P. de Silva, H. Q. N. Gunaratne, P. L. M. Lynch, G. E. M. Maguire and K. R. A. S. Sandanayake, Molecular fluorescent signalling with 'fluor–spacer–receptor' systems: approaches to sensing and switching devices via supramolecular photophysics, *Chem. Soc. Rev.*, 1992, **21**, 187; (*b*) A. P. de Silva, H. Q. N. Gunaratne, T. Gunnlaugsson, A. J. M. Huxley, C. P. McCoy, J. T. Rademacher and T. E. Rice, Signaling Recognition Events with Fluorescent Sensors and Switches, *Chem. Rev.*, 1997, **97**, 1515.

7 B. Valeur and I. Leray, Design principles of fluorescent molecular sensors for cation recognition, *Coord. Chem. Rev.*, 2000, **205**, 3.

8 Z. Xu, J. Yoon and D. R. Spring, Fluorescent chemosensors for $Zn^{2+}$, *Chem. Soc. Rev.*, 2010, **39**, 1996.

9 (*a*) E. M. Nolan and S. J. Lippard, Small-Molecule Fluorescent Sensors for Investigating Zinc Metalloneurochemistry, *Acc. Chem. Res.*, 2009, **42**, 193; (*b*) E. Tomat and S. J. Lippard, Imaging mobile zinc in biology, *Curr. Opin. Chem. Biol.*, 2010, **14**, 225.

10 K. P. Carter, A. M. Young and A. E. Palmer, Fluorescent Sensors for Measuring Metal Ions in Living Systems, *Chem. Rev.*, 2014, **114**, 4564.

11 N. C. Lim, J. V. Schuster, M. C. Porto, M. A. Tanudra, L. Yao, H. C. Freake and C. Brückner, Coumarin-Based Chemosensors for Zinc(II): Toward the Determination of the Design Algorithm for CHEF-Type and Ratiometric Probes, *Inorg. Chem.*, 2005, **44**, 2018.

12 K. Komatsu, Y. Urano, H. Kojima and T. Nagano, Development of an Iminocoumarin-Based Zinc Sensor Suitable for Ratiometric Fluorescence Imaging of Neuronal Zinc, *J. Am. Chem. Soc.*, 2007, **129**, 13447.

13 (*a*) L. Xue, H.-H. Wang, X.-J. Wang and H. Jiang, Modulating Affinities of Di-2-picolylamine (DPA)-Substituted Quinoline Sensors for Zinc Ions by Varying Pendant Ligands, *Inorg. Chem.*, 2008, **47**, 4310; (*b*) L. Xue, C. Liu and H. Jiang, A ratiometric fluorescent sensor with a large Stokes shift for imaging zinc ions in living cells, *Chem. Commun.*, 2009, 1061.

14 D. Bourassa, C. M. Elitt, A. M. McCallum, S. Sumalekshmy, R. L. McRae, M. T. Morgan, N. Siegel, J. W. Perry, P. A. Rosenberg and C. J. Fahrni, Chromis-1, a Ratiometric Fluorescent Probe Optimized for Two-Photon Microscopy Reveals Dynamic Changes in Labile Zn(II) in Differentiating Oligodendrocytes, *ACS Sens.*, 2018, **3**, 458.

15 Y. Wu, X. Peng, B. Guo, J. Fan, Z. Zhang, J. Wang, A. Cui and Y. Gao, Boron dipyrromethene fluorophore based fluorescence

Published on 20 2020. Downloaded on 17.10.2024 17:54:35.

sensor for the selective imaging of Zn(II) in living cells, *Org. Biomol. Chem.*, 2005, **3**, 1387.

16 S. C. Burdette, G. K. Walkup, B. Spingler, R. Y. Tsien and S. J. Lippard, Fluorescent Sensors for $Zn^{2+}$ Based on a Fluorescein Platform: Synthesis, Properties and Intracellular Distribution, *J. Am. Chem. Soc.*, 2001, **123**, 7831.

17 (*a*) J. C. Jeffery, C. R. Rice, L. P. Harding, C. J. Baylies and T. Riis-Johannessen, Ligand Reprogramming in Dinuclear Helicate Complexes: A Consequence of Allosteric or Electrostatic Effects? *Chem. – Eur. J.*, 2007, **13**, 5256; (*b*) S. Bullock, L. J. Gillie, L. P. Harding, C. R. Rice, T. Riis-Jojammessem and M. Whitehead, Isomeric pyridyl-thiazole donor units for metal ion recognition in bi- and tri-metallic helicates, *Chem. Commun.*, 2009, 4856.

18 M. H. Zheng, X. Hu, M. Y. Yang and J. Y. Jin, Ratiometically Fluorescent Sensing of Zn(II) Based on Dual-Emission of 2-Pyridylthiazole Derivatives, *J. Fluoresc.*, 2015, **25**, 1831.

19 M.-H. Zheng, J.-Y. Jin, W. Sun and C.-H. Yan, A new series of fluorescent 5-methoxy-2-pyridylthiazoles with a pH-sensitive dual-emission, *New J. Chem.*, 2006, **30**, 1192.

20 U.-W. Grummt, D. Weiss, E. Birckner and R. Beckert, Pyridylthiazoles: Highly Luminescent Heterocyclic Compounds, *J. Phys. Chem. A*, 2007, **111**, 1104.

21 M. J. Frisch, *et al.*, *Gaussian 16, Revision A.03*, Gaussian, Inc., Wallingford CT, 2016.

22 A. Hantzsch, Untersuchungen über Azole, *Justus Liebigs Ann. Chem.*, 1889, **250**, 257.

23 (*a*) E. Täuscher, D. Weiß, R. Beckert and H. Görls, Synthesis and Characterization of New 4-Hydroxy-1,3-thiazoles, *Synthesis*, 2010, 1603; (*b*) S. Wolfram, H. Würfel, S. H. Habenicht, C. Lembke, P. Richter, E. Birckner, R. Beckert and G. Pohnert, A small azide-modified thiazole-based reporter molecule for fluorescence and mass spectrometric detection, *Beilstein J. Org. Chem.*, 2014, **10**, 2470.

24 M. Kaufmann, M. L. Hupfer, T. Sachse, F. Herrmann-Westendorf, D. Weiß, B. Dietzek, R. Beckert and M. Presselt, Introducing double polar heads to highly fluorescent thiazoles: Influence on supramolecular structures and photonic properties, *J. Colloid Interface Sci.*, 2018, **526**, 410.

25 D. Aguila, E. Escribano, S. Speed, D. Talancon, L. Yerman and S. Alvarez, Calibrating the coordination chemistry tool chest: metrics of bi- and tridentate ligands, *Dalton Trans.*, 2009, 6610.

26 P. Suppan and N. Ghoneim, *Solvatochromism*, Royal Society of Chemistry, Cambridge, 1997.

27 T. Smith and J. Guild, The C.I.E. colorimetric standards and their use, *Trans. Opt. Soc.*, 1931, **33**, 73–134.

 This journal is © The Royal Society of Chemistry and the Chinese Chemical Society 2020